Frequency control support of a wind-solar isolated system by a hydropower plant with long tail-race tunnel

Guillermo Martínez-Lucas , José Ignacio Sarasúa, José Ángel Sánchez-Fernández, José Román Wilhelmi

Keywords:
Wind-solar-hydro systems
Pumped hydro storage system
Long tail-race tunnel
Speed governor tuning
Pole placement method
Root locus plot

A B S T R A C T

Pumped storage hydro plants (PSHP) can provide adequate energy storage and frequency regulation capacities in isolated power systems having significant renewable energy resources. Due to its high wind and solar potential, several plans have been developed for La Palma Island in the Canary archipelago, aimed at increasing the penetration of these energy sources. In this paper, the performance of the frequency control of La Palma power system is assessed, when the demand is supplied by the available wind and solar generation with the support of a PSHP which has been predesigned for this purpose. The frequency regulation is provided exclusively by the PSHP. Due to topographic and environmental constraints, this plant has a long tail-race tunnel without a surge tank. In this configuration, the effects of pressure waves cannot be neglected and, therefore, usual recommendations for PID governor tuning provide poor performance. A PI governor tuning criterion is proposed for the hydro plant and compared with other criteria according to several performance indices. Several scenarios considering solar and wind energy penetration have been simulated to check the plant response using the proposed criterion. This tuning of the PI governor maintains La Palma system frequency within grid code requirements.

1. Introduction

Generally, fossil fuels are very expensive in islands, principally because of transportation cost. Nevertheless, many islands have an excellent local wind and solar potential, so that economic, environmental and social costs of fuel electricity generation may be avoided. In last years, renewable energy sources have been used to substitute fossil fuels in small isolated systems [1–4].

One of the economic and technical drawbacks of the high participation of intermittent energy sources in isolated systems is the need to reject substantial amounts of the produced energy due to penetration limits in the local electric grids [5]. This affects to both, wind and PV generation.

The vast majority of studies agree that the introduction of storage systems is the most effective mean to significantly increase wind penetration levels in power system [5–8]. Pumped storage hydropower plans (PSHP) can contribute to this role, being able to compensate uncertainly in intermittent renewable energy (wind and solar). In fact, some current research is focused on the feasibility of the combination of solar, wind and hydro energy in islands (Fig. 1) [9]. This issue is also being considered in small isolated systems on some inland areas [10].

In some cases, sites available for building new PSHP may require long hydraulic conduits due to geographic, environmental or economic constraints. The main technical problem associated with long pipes is related to elastic phenomena, especially in those cases where for economic and environmental constraints no surge tank is built. In long pipelines, under-pressure and overpressure downstream or upstream of the turbine may result from the gate position movement. As an example, in long discharge pipes, cavitation phenomena may appear downstream the turbine due to an excessive suction pressure caused by gate closing movements [11].

The construction of a realistic model that takes into account all the phenomena involved in system operation is essential in order to draw relevant conclusions, applicable to predict the response of the station during design phase [12].

In particular, when the tail-race tunnel has a great length, the rigid-water-column models are not adequate [13] and consequently the controller settings based on it [14]. There are several researches which describe how to model the dynamic response

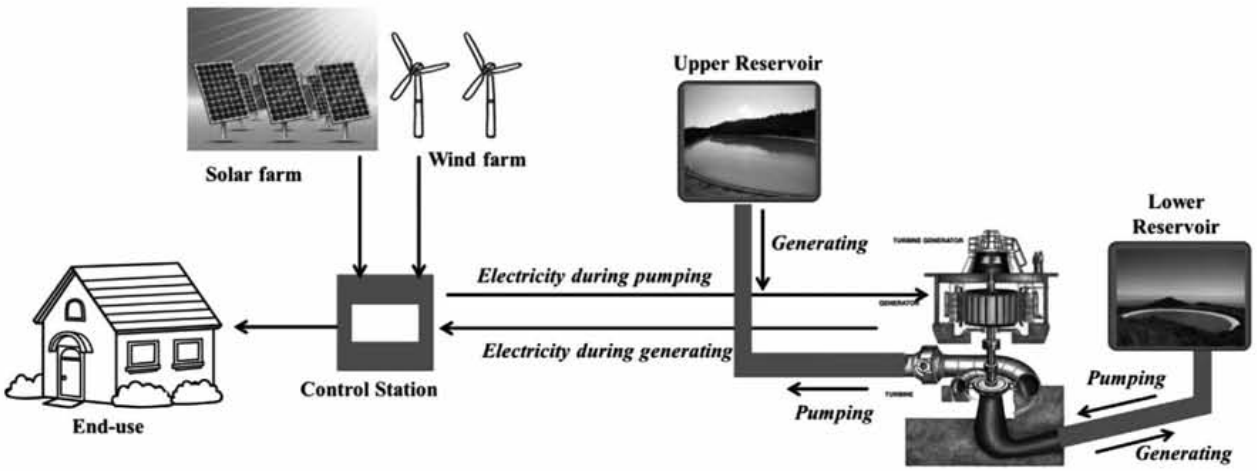

Fig. 1. A hybrid solar-wind system with pumped storage system.

when elastic phenomena cannot be neglected [15–19].

The use of PI controllers in hydropower plants to control speed governors is a usual practice [20] and several criteria for gain tuning have been developed in last decades [21–23]. Classic Control techniques, as root locus plot, have been successfully applied in order to obtain recommendations or expressions for PID speed governor tuning in the plant design phase [21,24–26], but this rules do not include water elasticity effects.

Regarding long pipes, very few studies have been found in the literature focused on the adjustment of PID governor gains in such cases. In Refs. [27], a hydropower plant with long penstock is modelled. In this study, authors propose two criteria to adjust PI gains assuming isolated system and wind energy penetration. In Refs. [28], a hydropower plant with long tail-race tunnel is modelled. In this case, the plant is aimed to contribute to secondary regulation.

La Palma is an island belonging to the Canary Islands archipelago and declared a Biosphere Reserve by UNESCO since 2002. Currently, the vast majority energy is provided by thermal plants, while only a small proportion is provided by wind and solar farms. The objective for next years is to reduce consumption of fossil fuel and increase the use of renewable resources [29]. For this purpose, it is expected to increase the installed capacity of wind and solar farms and to build a PSHP. One of the main objectives to be achieved is that at certain times, the energy is produced exclusively from renewable sources, thus overriding the thermal generation. In this case, the contribution of the hydropower plant to frequency regulation becomes very important, since the possible contribution of modern wind generators entails a cost: some wind energy will be lost [30].

In this paper, a PSHP in La Palma Island has been predesigned and modelled taking into account the penetration increasing rate of renewable energies (wind, solar and hydro) in recent years [31], as well as several published expansion plans [29–32].

In order to model the hydropower plant adequately, a detailed model which includes nonlinearities, head losses and distributed elasticity effects has been used. According to this aim, it is necessary to obtain the PI gains that allow to PSHP operate correctly. A methodology based on root locus plot to obtain these gains, taking into account water and tail-race tunnel elasticity effects has been developed. For this purpose, a simplified linearized model is obtained using the adjusted lumped parameter approach [16,17,27]. With this simplified model, an analysis in the frequency domain is developed, obtaining the transfer function of the control loop and the participation factor of each variable [18,23].

The adequacy of the proposed criterion for controller adjustment has been checked by comparison with other criteria, using some performance parameters belonging to the frequency and time domains (gain margin, phase margin, damping ratio…) as proposed in Ref. [33]. In order to evaluate the plant dynamic response due to different perturbations [34] (and its ability to operate in an isolated system with high penetration of solar and wind power) several simulations have been carried out. No contribution to frequency regulation from the wind farm has been considered.

The paper is organized as follows. In Section 2, the power system of La Palma Island (Canary archipelago) and the projected pumped storage hydropower plant are described. In Section 3, the hydropower plant dynamic model is presented, describing each element of the PSHP. In Section 4, a reduced order model is used in order to analyze the system in frequency domain. In Section 5, a tuning criterion based on root locus method is formulated, being compared with others classic ones. In Section 6, some real cases are proposed in order to simulate the PSHP dynamic response with the tuning criterion proposed. Finally, in Section 7 main conclusions of the paper are properly summarized.

2. Power system and PSHP description

The amount of electrical energy generated in 2013 on the island of La Palma was 262,375 MWh of which only 9.1% came from renewable sources, while the remaining 90.9% was produced by fossil fuels. The maximum peak demand for that year was 42 MW [31]. In order to reduce the share of fossil fuels, the authorities of the island of La Palma intend to carry out a major project to increase the penetration of renewable energy [35].

Currently, the installed generation capacity from fossil fuels is 82.8 MW in diesel generators and 22.5 MW in gas turbines. The renewable sources are shown in Fig. 2, including four wind farms (W) distributed throughout the island with an installed capacity of 9 MW and two solar photovoltaic (Pv) plants with an installed capacity of 4.9 MW [31]. In the last years, several expansion plans have been developed in order to increase the penetration of renewable energy throughout the archipelago [29,32]. According to the penetration rate of these energies in recent years [31] and taking into account the development plans of the energy system [32] it is considered that the most likely action would be to install a wind farm of about 20 MW. In this scenario, it would be necessary to have sufficient power regulation capacity in a pumped storage hydroelectric plant (PSHP) for integration of the other renewable energy sources [35,36].

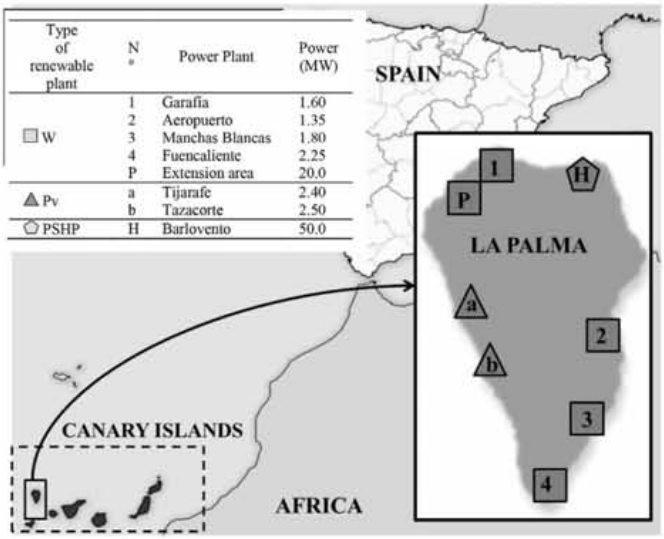

Fig. 2. Geographical location of La Palma island in the Canary Archipelago, and its renewable power plants.

The PSHP is to be placed in the northeast area of the island, using as lower reservoir an existing irrigation pond, Barlovento, which has excess of capacity for the current demand. According to the expansion plan, the upper reservoir would be placed in Las Cancelitas (Fig. 3). Published studies are preliminary in a very basic level, so it was considered necessary to complete them; thus, the PSHP was pre-dimensioned to carry out the present study.

The power plant will have two 25 MW pump-turbines. The powerhouse will be placed in a cavern under the valley between "Las Cancelitas" and "El Lomito" where the tail-race tunnel starts. As it is shown in Figs. 3 and 4, the tail-race conduit runs from this point, under the rock masses of "El Lomito" and "Llanadas de Verone" to the lower reservoir of Barlovento. The characteristics of the PSHP are summarised in Table 1. A preliminary assessment has shown that this PSHP together with wind and solar power would supply the demand at some time intervals without the contribution of fossil fuel power plants.

3. Simulation model

The electric power system of La Palma Island has been modelled as an isolated system, where the PSHP would be the only generation plant supplying the *net demand*, i.e. the residual demand remaining after subtracting the intermittent wind and solar generation. This hypothesis implies that wind and solar generation do not contribute to frequency regulation; this service being exclusively provided by the PSHP plant. Therefore, according to work's objectives, PSHP will operate in generation mode during all simulations.

In this study, a hydroelectric plant with a long tail-race conduit is modelled. A PI controller, the penstock and the tail race are included in the model. Elastic effects are considered only in the tail-race. Fig. 5 shows the main blocks of the model and their interconnections. The equations associated with each block are detailed in the following sections. All variables are expressed in per unit.

3.1. Penstock

Due to its short length, penstock is modelled assuming the rigid water column approach, including water inertia and head losses [15,37]. Thus, the penstock dynamics is given by Equation (1).

$$\frac{dq_p}{dt} = \frac{1}{T_{wp}}\left(h_c - h - h_t - \frac{r_p}{2}\cdot q_p \cdot \left|q_p\right|\right) \tag{1}$$

where T_{wp} is the penstock water starting time and it is defined as (2):

$$T_{wp} = \frac{L_p}{gF_p}\frac{Q_b}{H_b} \tag{2}$$

The relationship between turbine pressures up-stream and down-stream and net head is shown in Fig. 4 and is expressed by (3):

$$h = h_p - h_t \tag{3}$$

Water level variations in both reservoirs are neglected due to their very large time constant.

3.2. Turbine

Turbine operation is described by two functions. First function relates flow with net head and wicket-gate position. The second one relates the generated power with the flow, net head, gate position and speed. This model is recommended in Ref. [15] and the expressions are (4) and (5)

$$q = z\sqrt{h} \tag{4}$$

$$p_g = A_t h(q - q_{nl}) - Dz\Delta n \tag{5}$$

The modelled power plant has two identical units, which are supposed to work at the same operating point. Thus, a single equivalent turbine has been considered.

3.3. Generator and external system

As stated above, the hydro power plant is connected to an isolated system comprising intermittent energy sources and loads. Intermachine mechanical oscillations will be neglected, so that the frequency is represented by a unique value; then, the frequency dynamics (6) results from the imbalance between generator power, p_g and net demand, p_d [12,38,39].

$$p_g - p_d - k\Delta n = (T_m + T_{ps})n\frac{dn}{dt} \tag{6}$$

where inertia mechanical starting time, T_m, corresponds to the hydro plant and T_{ps}, corresponds to the inertia of rotating loads; wind an PV generation have been included in p_d as a negative demand; wind generators are supposed to be connected to the system through frequency converters and do not contribute to system inertia. The parameter k includes only load frequency sensitivity effects, as it has been assumed that wind and solar generation do not contribute to frequency regulation.

3.4. PI controller

A conventional proportional-integral (PI) controller processes the frequency error signal $(n_{ref} - n) - \sigma z$. Equation (7) gives the changes in the gate position due to the controller action [14].

$$z = \left[\frac{1}{\delta} + \frac{1}{\delta T_r}\int dt\right]\left[\left(n_{ref} - n\right) - \sigma z\right] \tag{7}$$

The PI gains are:

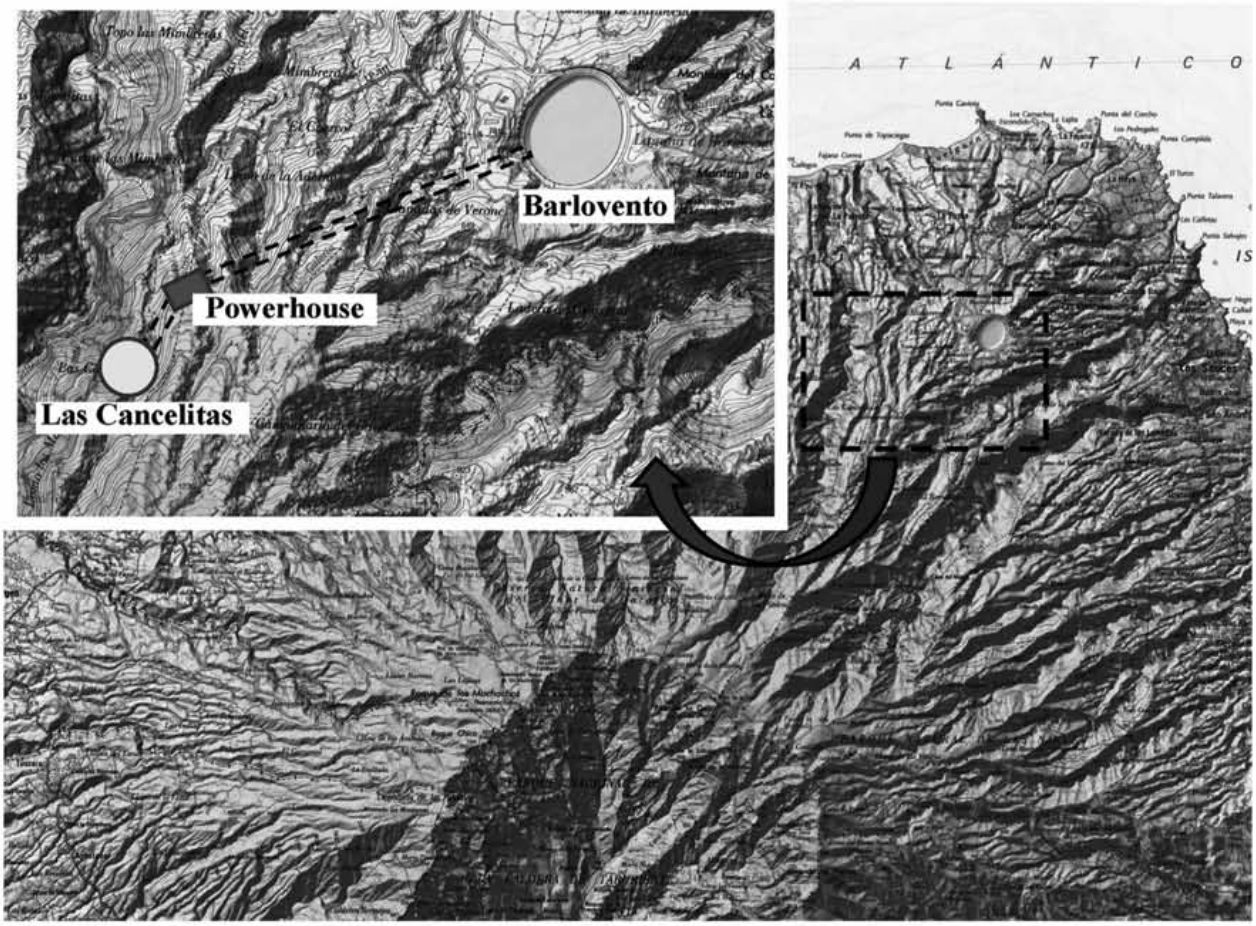

Fig. 3. PSHP layout.

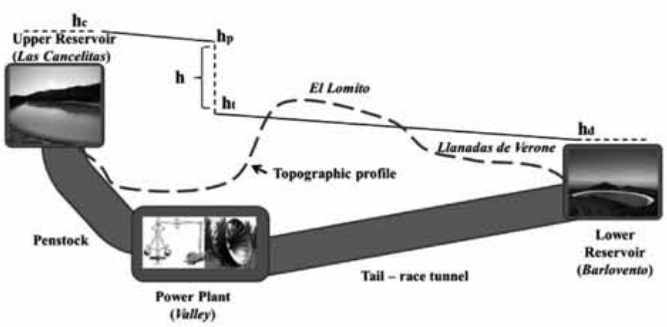

Fig. 4. Plant and topography profile schemes.

Table 1
Barlovento hydro power plant main data.

Power plant		Penstock		Tail-race tunnel	
H	304 m	L_p	550 m	L_d	1950 m
Q	17.8 m^3/s	D_p	2.00 m	D_d	2.50 m
P	50 MW	v_p	5.67 m/s	v_d	3.63 m/s

$$K_P = \frac{1}{\delta} \text{ y } K_I = \frac{1}{\delta T_r} \tag{8}$$

As it is shown in Fig. 6, the gate movement has a rate limiter (±0.1 p.u./s) and a minimum and a maximum position [15]. These

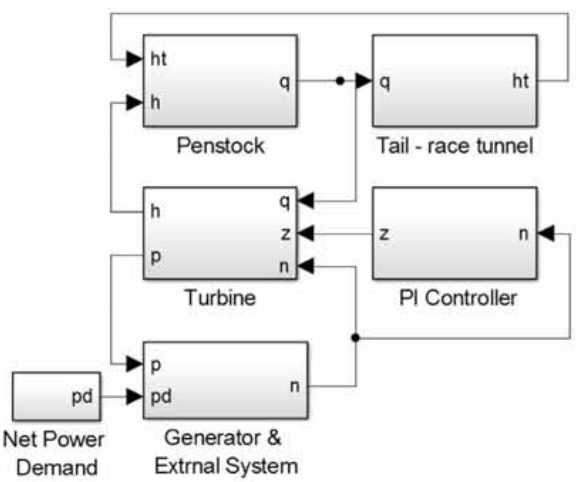

Fig. 5. Block diagram of the plant model.

non-linear elements can affect the response to a great perturbation. However, they have not been considered in the analytical study because it is based on a small perturbation linearized model.

3.5. Tail-race

In order to consider water and conduit elasticity, expression (9) is used [27].

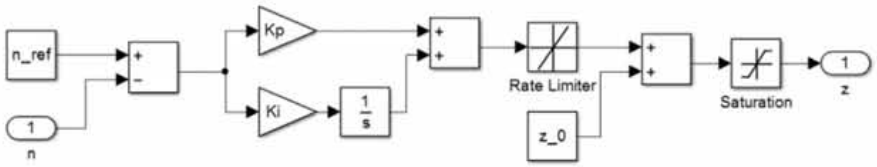

Fig. 6. Block diagram of PI controller.

$$\frac{\Delta H_t(s)}{\Delta Q_d(s)} = -\frac{T_{wd}\frac{a_d}{L_d}\left(1 - e^{-2\frac{L_d}{a_d}s}\right)}{1 + e^{-2\frac{L_d}{a_d}s}} \tag{9}$$

The head losses, $(r_d/2)$, are included as shown in Fig. 7 [15].

4. Reduced order model

For control design purposes in plants with long conduits, it is convenient in general to use a reduced order model including elasticity effects [20]. In this case, it has been considered necessary only in the tail-race tunnel.

4.1. Lumped parameters approach

In last years some authors [16,40,41] have obtained good results with their hydro power plant models, representing penstock elasticity effects by means of several consecutive elements, where the conduit properties, inertia, elasticity and friction, are assigned proportionally to the segment length. Accordingly, long conduits can be modelled considering the lumped parameter approach. In Ref. [27] it has been verified that the simplest model, one Π-shaped segment model having one series branch and two shunt branches can be accurate enough. Here, tail-race tunnel will be modelled assuming these guidelines. Since the height at the downstream end of tail-race can be considered as constant, a second order model will result, (10) and (11):

$$\frac{dq_d}{dt} = \frac{1}{T_{wd}}\left(h_t - h_d - \frac{r_d}{2}\cdot q_d \cdot |q_d|\right) \tag{10}$$

$$\frac{dh_t}{dt} = \frac{2T_{wd}}{\beta T_{ed}^2}\left(q_p - q_d\right) \tag{11}$$

The single Π-shaped segment-model is corrected through the coefficient β [27]. The correction coefficient β is adjusted so that the natural frequency of the one-segment transfer function matches the first peak of the frequency response of continuous model (9).

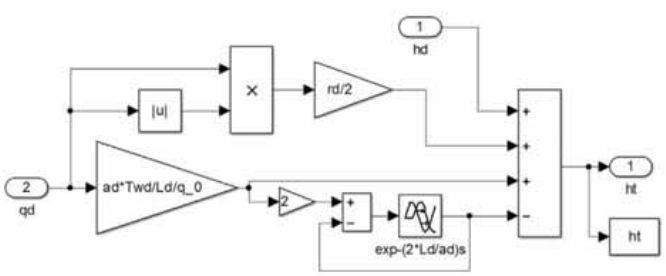

Fig. 7. Block diagram of tail race.

4.2. Linearization

Some of the components described above are represented by nonlinear expressions and, therefore, are not suitable for adjustment of the controller using linear methods. Thus, a linearized model is derived for small perturbation analysis in the neighbourhood of an initial equilibrium operating point.

The equations that characterize the hydro power plant are (1), (4)–(7), (10) and (11), where nonlinearities appear in the inertial penstock equation, (1) in the turbine Equations (4) and (5) and in the inertial tail-race Equation (10).

4.2.1. Turbine

The linearized model of a hydraulic turbine can be written as follows:

$$\Delta q_p = b_{11}\Delta h + b_{12}\Delta n + b_{13}\Delta z \tag{12}$$

$$\Delta c_t = b_{21}\Delta h + b_{22}\Delta n + b_{23}\Delta z \tag{13}$$

$$\Delta p_g = n^0 b_{21}\Delta h + \left(n^0 b_{22} + c_t^0\right)\Delta n + n^0 b_{23}\Delta z \tag{14}$$

The coefficients b_{1i} are the partial derivatives of the water flow (4) with respect to net head, speed and wicket gate position whereas than the coefficients b_{2i} are the partial derivatives of the torque (5) with respect to the same variables. Both groups of coefficients are expressed in (15).

$$b_{11} = \left.\frac{\partial q_p}{\partial h}\right|_{(h,n,z)^0} = \frac{z^0}{2\sqrt{h^0}} \qquad b_{21} = \left.\frac{\partial c_t}{\partial h}\right|_{(h,n,z)^0} = \frac{A_t}{n^0}\left(\frac{z^0}{2}\sqrt{h^0} + q_p^0 - q_{nl}\right)$$
$$b_{12} = \left.\frac{\partial q_p}{\partial n}\right|_{(h,n,z)^0} = 0 \qquad b_{22} = \left.\frac{\partial c_t}{\partial n}\right|_{(h,n,z)^0} = -\frac{1}{n^0}\left(Dz^0 + c_t^0\right)$$
$$b_{13} = \left.\frac{\partial q_p}{\partial z}\right|_{(h,n,z)^0} = \sqrt{h^0} \qquad b_{23} = \left.\frac{\partial c_t}{\partial z}\right|_{(h,n,z)^0} = \frac{A_t}{n^0}\left(h^0\right)^{\frac{3}{2}} \tag{15}$$

4.2.2. Penstock

Linearizing the friction losses term in the penstock equation (1), and taking into account the head relations (3), results in (16):

$$\frac{d\Delta q_p}{dt} = \frac{1}{T_{wp}}\left[-\left(\frac{1}{b_{11}} + r_p q_p^0\right)\Delta q_p - \Delta h_t + \frac{b_{12}}{b_{11}}\Delta n + \frac{b_{13}}{b_{11}}\Delta z\right] \tag{16}$$

4.2.3. Tail-race

Likewise the above section, linearizing tail-race Equation (10) results in (17):

$$\frac{d\Delta q_d}{dt} = \frac{1}{T_{wd}}\left(\Delta h_t - r_d q_d^0 \Delta q_d\right) \tag{17}$$

4.3. Frequency domain analysis

The objective of the frequency domain analysis is to obtain the transfer function which relates the frequency variation with the demanded power. Perturbation input (net demanded power, P_d) is only considered because the reference frequency, n_{ref}, should remain constant due to the controller objective: to maintain constant system frequency.

To determinate this function, the penstock (16) and the elastic tail – race expressions (11) and (17) are formulated in the frequency domain, subsequently combining them with the turbine flow Equation (12) to obtain the variations in the tail-race flow in terms of the variations in speed and wicket gates position:

$$\Delta Q_p(s) = \frac{\left(\beta T_{ed}^2 s\left(sT_{wd} + r_d q_d^0\right) + 2T_{wd}\right)\left(b_{12}\Delta N(s) + b_{13}\Delta Z(s)\right)}{\left(\left(\beta T_{ed}^2 s\left(sT_{wd} + r_d q_d^0\right) + 2T_{wd}\right)\left(sT_{wp} + \frac{1}{b_{11}} + r_p q_p^0\right) + 2T_{wd}\left(sT_{wd} + r_d q_d^0\right)\right) b_{11}} \tag{18}$$

Taking into account Equation (14), changes in the output power, $\Delta P_g(s)$, can be expressed as:

$$\Delta P_g(s) = \left[\frac{b_{21}\left(\beta T_{ed}^2 s\left(sT_{wd}+r_d q_d^0\right)+2T_{wd}\right)\left(b_{12}\Delta N(s)+b_{13}\Delta Z(s)\right)}{b_{11}^2\left(\left(\beta T_{ed}^2 s\left(sT_{wd}+r_d q_d^0\right)+2T_{wd}\right)\left(sT_{wp}+\frac{1}{b_{11}}+r_p q_p^0\right)+2T_{wd}\left(sT_{wd}+r_d q_d^0\right)\right)}\right] + \left(b_{22}+\frac{c_t^0}{n^0}-\frac{b_{21}b_{12}}{b_{11}}\right)\Delta N(s) + \left(b_{23}-\frac{b_{21}b_{13}}{b_{11}}\right)\Delta Z(s) \tag{19}$$

And it can be reformulated as:

$$\Delta P_g(s) = G_N(s)\Delta N(s) + G_Z(s)\Delta Z(s) \tag{20}$$

where:

$$G_N(s) = \frac{b_{21}b_{12}}{b_{11}^2}\frac{\left(\beta T_{ed}^2 s\left(sT_{wd} + r_d q_d^0\right) + 2T_{wd}\right)}{\left(\beta T_{ed}^2 s(sT_{wd} + r_d q_{d0}) + 2T_{wd}\right)\left(sT_{wp} + \frac{1}{b_{11}} + r_p q_p^0\right) + 2T_{wd}\left(sT_{wd} + r_d q_d^0\right)} + b_{22} + \frac{c_{t_0}}{n_0} - \frac{b_{21}b_{12}}{b_{11}} \tag{21}$$

$$G_Z(s) = \frac{b_{21}b_{13}}{b_{11}^2}\frac{\left(\beta T_{ed}^2 s\left(sT_{wd} + r_d q_d^0\right) + 2T_{wd}\right)}{\left(\beta T_{ed}^2 s\left(sT_{wd} + r_d q_d^0\right) + 2T_{wd}\right)\left(sT_{wp} + \frac{1}{b_{11}} + r_p q_p^0\right) + 2T_{wd}\left(sT_{wd} + r_d q_d^0\right)} + b_{23} - \frac{b_{21}b_{13}}{b_{11}} \tag{22}$$

The frequency dynamics Equation (6) is now formulated in frequency domain resulting in:

$$\Delta P_g(s) - \Delta P_d(s) - k\Delta N(s) = \left(T_m + T_{ps}\right) n^0 s \Delta N(s) \tag{23}$$

Controller transfer function, G_C, describes speed governor dynamics in frequency domain.

$$G_C = \frac{\Delta Z(s)}{-\Delta N(s)} = \frac{1 + T_r s}{\delta T_r s} \tag{24}$$

Finally, combining expressions (20), (23) and (24), the system transfer function results:

$$\frac{-\Delta N(s)}{\Delta P_d(s)} = \frac{1}{\left(T_m + T_{ps}\right) n^0 s + k - G_N(s) + G_Z(s)G_C(s)} \tag{25}$$

5. Proposed PI tuning criteria

Three different criteria are described for tuning the PI governor of the speed control loop of hydroelectric power plants with long tail-race tunnel operating in an isolated system. The first one, Double Complex Pole (DCP) is taken from Ref. [27]. The second one, Fixed Damping Ratio (FDR) is taken from Ref. [42]. The third one is referred to Fixed Damping Ratio Modified (FDRM) since it is based on FDR where some modifications have been introduced.

Table 2
Nominal operating point values (p.u.).

q_p^0	1.0	q_d^0	1.0	h^0	1.0
n^0	1.0	c_t^0	1.0	z^0	1.0
p_g^0	1.0	A_t	1.0526	q_{nl}	0.050
D	2.00	$r_p/2$	0	$r_d/2$	0

The first two criteria are based on fourth order models, due to they were developed to control speed governors in hydropower plants with long penstock, so it has been necessary to adapt them to the case study. The third one is formulated for a fifth order model of a hydropower plant with long tail-race tunnel.

All of them are based on a root locus analysis of the simplified speed control loop. In last years, many works based on the root locus technique to adjust speed governors have been developed [43,24].

Table 3
Barlovento hydropower plant time constants.

T_{wp}	0.9927 s
T_{wd}	2.2525 s
T_{ed}	1.9500 s
$T_m + T_{ps}$	6.00 s
k	0

For tuning purposes, only, friction losses ($r_p/2$ and $r_d/2$) are neglected [44]. The plant is supposed to operate in rated conditions. The parameters of expression (5) have been taken from Ref. [45]. The numerical values of the PSHP are collected in Table 2.

5.1. Double Complex Pole (DCP)

According to this criterion, developed for a PSHP with long penstock in an isolated system [27], the two pairs of complex poles of the control loop are forced to have the same value. DCP criterion was formulated considering a Pelton turbine, which has different coefficients b_{2j}. For this reason, the equations system presented in Ref. [27] has been re-formulated considering the b_{2j} coefficients indicated in Table 2. Further, in this case, it is necessary to consider the tail-race tunnel inertia. Then, a global water starting time ($T_w = T_{wp} + T_{wd}$) has been used to represent the inertia of the conduits (penstock and tail-race tunnel).

This criterion was designed for a fourth-order system, so in the fifth-order system the poles cannot be located in general at the same place; then, the slower pole pair is placed as far as possible from the imaginary axis. Given the time constants listed in Table 3, the resulting values of the controller gains and the poles of the closed loop transfer function are shown in Table 4. The root locus plot with the poles position highlighted is represented in Fig. 8.

5.2. Fixed Damping Ratio (FDR)

In Ref. [22] authors recommend using the $\zeta = 0.707$ damping

Table 4
PI parameters, closed-loop poles, participation factor modules (p.u.) of variables in response modes, corresponding to each proposed criteria.

Criteria	PI parameters		Closed loop poles	Participation factor module (p.u.)					Response mode
	δ (p.u.)	T_r (s)		q_p	q_d	h_t	n	Z	
DCP	1.8169	2.9952	−0.6536 ± j1.0594	0.3338	0.1661	0.3967	0.0001	0.1033	A
			−0.2587 ± j0.1144	0.1699	0.3265	0.0402	0.0037	0.4596	B
			−0.34	0.0724	0.1184	0.0211	0.6428	0.1452	C
FDR	2.3618	8.0769	−0.6464 ± j0.9891	0.3128	0.1819	0.3914	0.0200	0.0939	A
			−0.4437 ± j0.3559	0.1854	0.2871	0.1432	0.1540	0.2304	B
			−0.0266	0.0283	0.0641	0.0001	0.1430	0.7646	C
FDRM	1.4552	3.2272	−0.6962 ± j1.1107	0.3572	0.1421	0.3763	0.0027	0.1216	A
			−0.2422 ± j0.2422	0.1539	0.3381	0.0611	0.0491	0.3977	B
			−0.2422	0.1112	0.2122	0.0192	0.3154	0.3421	C
Paynter	1.3522	16.226	−0.7757 ± j1.1334	0.3757	0.1161	0.3374	0.0318	0.1389	A
			−0.2655 ± j0.4676	0.1088	0.3328	0.1483	0.1547	0.2553	B
			−0.0192	0.0182	0.0412	0	0.2641	0.6765	C

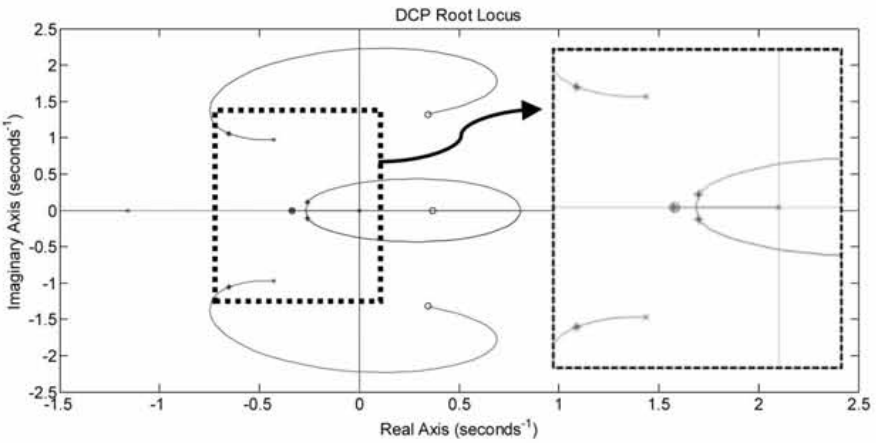

Fig. 8. Root Locus Barlovento hydropower plant in isolated operation with DCP.

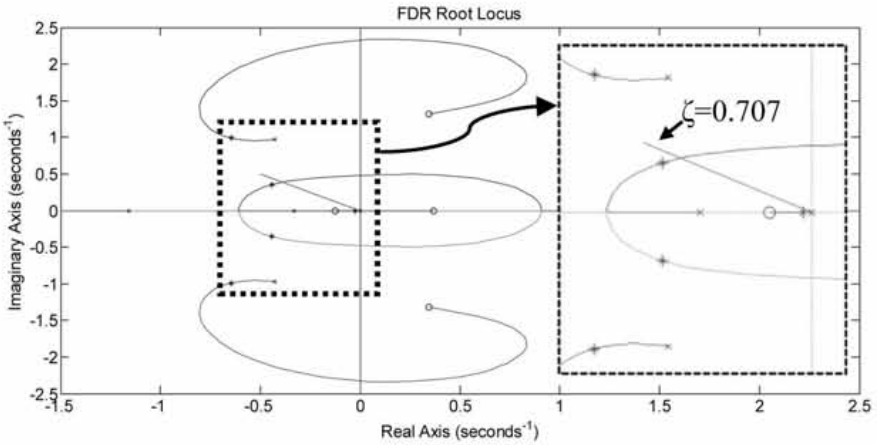

Fig. 9. Root Locus Barlovento hydropower plant in isolated operation with FDR.

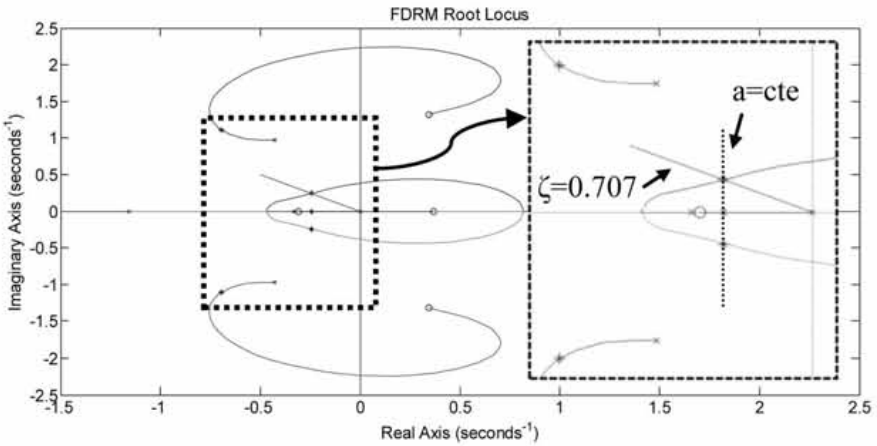

Fig. 10. Root Locus Barlovento hydropower plant in isolated operation with FDRM criterion.

ratio as design criterion. This criterion has been applied in Refs. [42], where the authors propose some abacuses and approximate expressions to obtain the controller parameters, T_r and δ $(1/K_p)$ in terms of plant time constants, T_m, T_e and T_w. These expressions are based on a fourth order model with a long penstock. In this work, for long discharge tubes, the total starting time ($T_w = T_{wp} + T_{wd}$) and the elastic time constant of the discharge pipe ($T_e = T_{ed}$) have been considered. The resulting controller parameters are given in this case by (26) and (27):

$$T_r = 0.64(T_{wp} + T_{wd}) + T_m \tag{26}$$

$$\delta = 0.09\left(\frac{(T_{wp} + T_{wd})T_{ed}}{T_m}\right)^2 + 0.03\frac{(T_{wp} + T_{wd})T_{ed}}{T_m} + 2.23 \tag{27}$$

The values of the controller gains for the time constants listed in Table 3 and the poles of the closed loop transfer function are shown in Table 4. Note that controlled poles are λ_4 and λ_5. Also, the root locus and poles location are shown in Fig. 9, which shows that a couple of poles are located near the line of fixed damping. The differences found are due to applying a criterion based on a fourth order model to a fifth order model.

5.3. Fixed Damping Ratio Modified (FDRM)

The plant model in study is of fifth order, so there are 5 poles. At least, one of these poles is on the real axis. The condition imposed by the previous criterion on the mechanical-water pole ($\zeta = 0.707$) may remain in force, but now a condition should be imposed to the real pole. As discussed in Refs. [25,27], the tuning criterion influences the controlled variable settling time. Specifically, it reduces it by increasing the pole real part (in absolute value). This consideration implies having a lower settling time, at the expense of the overshoot.

According to this criterion, the five generic transfer function poles are forced to be of the form $\{a, a\pm ja, b\pm jc\}$; so, the closed loop transfer function denominator can be written as (28).

$$(x-a)(x-(a-ja))(x-(a+ja))(x-(b-jc))(x-(b+jc)) \tag{28}$$

Then, the closed loop poles are given by the solution of a fifth order equation system (29), where the five unknown variables are: a, b, c, K_p and Tr.

$$\frac{2T_{wp}+2T_m+kT_{wp}-2T_{wp}K_p}{(T_m+T_{ps})T_{wp}}=-3a-2b$$

$$\frac{4T_rT_{ed}^2+2kT_rT_{ed}^2-2K_pT_{ed}^2T_{wp}+2.1051T_rK_pT_{ed}^2+2.4673T_rT_m(T_{wp}+T_{wd})}{(T_m+T_{ps})T_rT_{wp}T_{ed}^2}=4a^2+6ab+b^2+c^2$$

$$\frac{4.9348T_r(T_{wp}+T_{wd}-K_p(T_{wp}+T_{wd})+T_m+T_{ps})+2.4674kT_r(T_{wp}+T_{wd})+2.1052T_{ed}^2K_p}{(T_m+T_{ps})T_rT_{wp}T_{ed}^2}=-a\left(2a^2+8ab+3b^2+3c^2\right) \quad (29)$$

$$\frac{9.8692T_r-4.9346K_p(T_{wp}+T_{wd})+5.1942T_rK_p+4.9348kT_r}{(T_m+T_{ps})T_rT_{wp}T_{ed}^2}=4a^2\left(ab+b^2+c^2\right)$$

$$\frac{5.194177K_p}{T_r(T_m+T_{ps})T_{wp}T_{ed}^2}=2a^3\left(-b^2-c^2\right)$$

The essential parameters of the plant under study are the time constants listed in Table 3. Poles of the closed loop transfer function are shown in Fig. 10.

It is supposed that loads connected to the power plant are resistive, as it is usual in power plants connected to isolated systems [33].

5.4. Modal analysis

The controller parameters obtained using the previously described criteria are summarized in Table 4, along with the corresponding closed loop poles of the speed control loop. The participation factors of each variable have been determined by means of a modal analysis [23]. These columns express the module of the participations factors of each variable in each oscillation mode in relative terms. In order to determine the variables prevailing in each mode, it has been used the rule developed in Refs. [18], assuming that the sum of the participation factor module of the predominant variables should be greater than 0.8. At the same time, it has been considered appropriate to compare the proposed criteria with a classic criterion [46].

In all cases the fifth-order system, shows two oscillatory modes and one exponential mode. In the first of them, A, clearly present in all settings, the predominant variables are *qp*, *qd* and *ht*; it is the elastic mode [18], on which any condition has been imposed. In the second one, B, it can be distinguished two different modal shapes; on the one hand, criteria DCP and FDRM present greater influence the variables *qd* and *z*; while on the other hand, in FDR and Paynter criteria there are no predominant variables. This behaviour may be related to the settling time control in DCP and FDRM criteria. Also, this similarity in the oscillation modes in pairs will be also observed in Fig. 11 and Fig. 14. Finally, in the oscillation mode C prevails in all cases the variables *n* and *z*, thus it is a mechanic-water mode.

5.5. Evaluation of the proposed tuning criteria

In order to evaluate and compare the different tuning criteria, some performances indices for governor control systems proposed in Ref. [33] have been used. The numerical values of these indices corresponding to each tuning criterion are obtained from the complete simulation model, including head losses, and given in Table 5.

Fig. 11 shows the hydro power plant response due to a unit impulse, considering all the proposed tuning criteria and the classic Paynter criterion. It can be seen, as given in the previous table, that DCP and FDRM have much lower settling times than FDR and Paynter criteria, while there are not significant differences in the maximum peak values.

6. Simulations and results

In most power systems, the main contribution to frequency

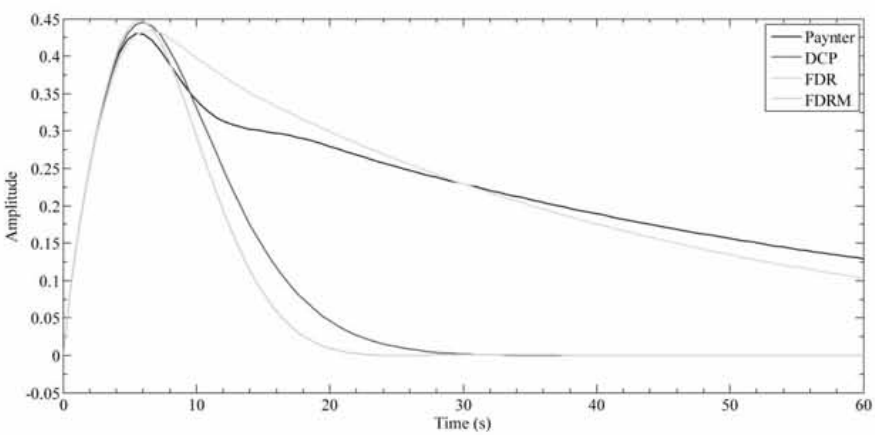

Fig. 11. Hydro plant dynamic response due to a unit impulse using Paynter, DCP, FDR and FDRM Criteria.

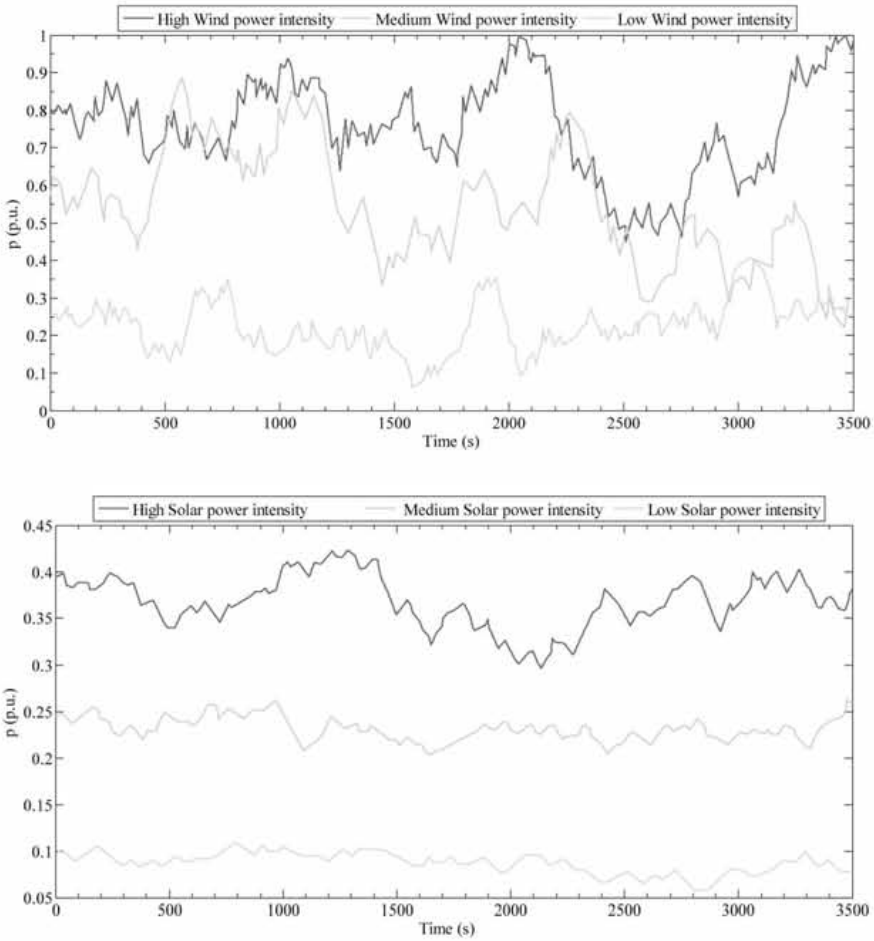

Fig. 12. Wind and solar power output.

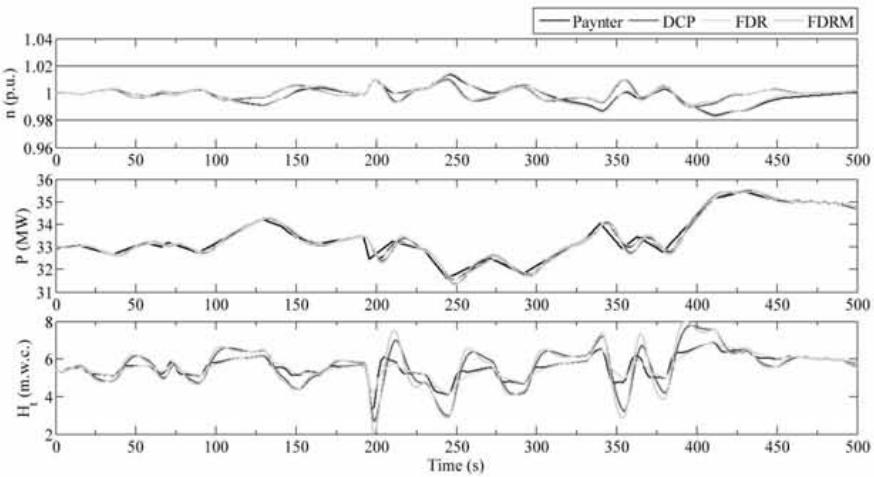

Fig. 13. 500 s simulation of PSHP with high penetration of wind and solar energy (H−H).

regulation corresponds to thermal power plants. However, in the system studied here this service is uniquely provided by the PSHP which should compensate the fluctuations of wind and solar energy. Then, one of the main functions of PSHP is to maintain the system frequency within the power quality limits according to regulation [47]. Two different limits are established for non-interconnected supply systems: 50 Hz ± 2% for 95% and 50 Hz ± 15% for 100% of a week.

Due to the long tail-race tunnel cavitation phenomena can appear downstream of the turbine. To avoid this harmful effect, the absolute pressure at that point should be greater than the vapour pressure [48]. In this case, this is equivalent to keep the relative pressure downstream of the turbine greater than −10 m of water column.

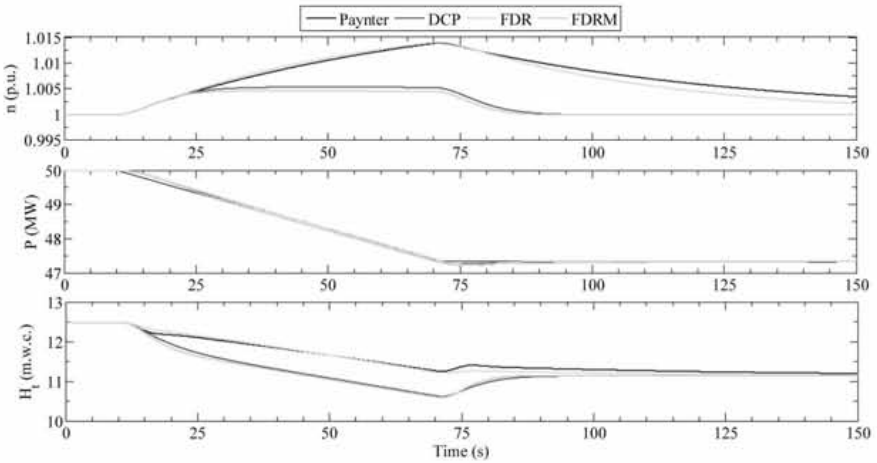

Fig. 14. Hydro plant response due to a power ramp.

Table 5
Performance indices for different tuning criteria for reference power plant.

Performance index	DCP	FDR	FDRM	Paynter	IEEE recommendations	
					Typical ranges	Good performance
Gain margin (dB)	3.8029	6.3540	4.2005	6.6702	2.0–20	3
Phase margin (dB)	39.0357	88.3593	44.0564	104.9461	20–80	40
Mp	0.6484	0.4673	0.6842	0.4567	1–4	1.1–1.6
Settling time (s)	25.7094	152.9497	20.0814	201.1503	2–100	
Damping ratio	0.9146	0.780	0.707	0.494	0.25–1	0.6–1

Table 6
Response quality parameters due to wind and solar power fluctuations (Low, Medium and High).

Setting		Criteria	Quality parameters				
Wind	Solar		$\overline{\sum \varepsilon_n^2} \times 10^{-5}$	$\overline{\sum \varepsilon_p^2} \times 10^{-5}$	$desv_{n.max}{}^{+}$ (%)	$desv_{n.max}{}^{-}$ (%)	$H_{t.\,min}$ (m)
L	L	Paynter	2.4371	0.2540	1.5609	−1.4760	8.8985
		DCP	0.7335	0.3694	0.7058	−0.8045	8.3211
		FDR	2.4999	0.2837	1.5537	−1.5259	8.9740
		FDRM	0.6144	0.3822	0.6885	−0.7370	8.1874
L	M	Paynter	2.5480	0.2617	1.6133	−1.5635	8.1186
		DCP	0.7379	0.3840	0.7716	−0.8293	7.5771
		FDR	2.6053	0.2929	1.5964	−1.6083	8.2429
		FDRM	0.6168	0.3985	0.7179	−0.7580	7.4338
L	H	Paynter	2.7569	0.2825	1.4438	−1.6785	7.4422
		DCP	0.7927	0.4224	0.7898	−0.8048	6.9604
		FDR	2.8171	0.3196	1.4631	−1.6009	7.5010
		FDRM	0.6613	0.4364	0.7585	−0.7417	6.7756
M	L	Paynter	6.9132	0.4830	2.0333 (*)	−2.0257 (*)	5.2115
		DCP	1.5629	0.6693	1.6520	−1.3103	3.5297
		FDR	6.8367	0.5588	2.0130	−2.0118 (*)	5.5169
		FDRM	1.2640	0.6706	1.5794	−1.3013	3.0821
M	M	Paynter	6.9758	0.5019	1.9717	−2.0755 (*)	4.5720
		DCP	1.5766	0.7064	1.5941	−1.2919	2.9031
		FDR	6.9182	0.5840	1.9520	−2.0243 (*)	4.8907
		FDRM	1.2734	0.7080	1.5552	−1.2907	2.4406
M	H	Paynter	7.1814	0.5340	2.1593 (*)	−2.1154 (*)	3.7422
		DCP	1.6349	0.7652	1.7867	−1.3873	1.8320
		FDR	7.1296	0.6281	2.3020 (*)	−2.1768 (*)	4.0772
		FDRM	1.3181	0.7654	1.6905	−1.3734	1.3531
H	L	Paynter	4.7002	0.8076	2.0094 (*)	−1.9522	3.8903
		DCP	1.8447	1.4403	1.7093	−1.6302	2.7923
		FDR	4.8006	0.9314	2.1303 (*)	−1.9885	4.5961
		FDRM	1.5763	1.4709	1.6177	−1.5761	2.1626
H	M	Paynter	4.7934	0.8463	2.1072 (*)	−1.9287	3.2578
		DCP	1.9219	1.5416	1.7339	−1.6948	2.0148
		FDR	4.9441	0.9839	2.2584 (*)	−2.0650 (*)	3.9907
		FDRM	1.6366	1.5700	1.6797	−1.6362	1.3475
H	H	Paynter	4.7541	0.8946	2.1369 (*)	−1.9436	2.6824
		DCP	2.0240	1.6742	1.6958	−1.7374	1.3574
		FDR	4.9887	1.0515	2.2853 (*)	−2.0678 (*)	3.4608
		FDRM	1.7169	1.6957	1.6010	−1.6740	0.6719

(*) marks the frequency deviations exceeding system requirements. Adjustments based on FDRM and DCP criteria do not fail in any of the cases provided. None of the cases compromises the security of the pipeline due to cavitation problems.

Table 7
Response quality parameters due to a ramp in wind power production.

Criteria	Quality parameters			
	$\overline{\sum \varepsilon_n^2} \times 10^{-6}$	$\overline{\sum \epsilon_p^2} \times 10^{-7}$	$desv_{n,max}{}^{+}$	$T_{2\%}{}^{n}$ (s)
Paynter	34.97	6.33	1.39%	150.22
DCP	5.00	3.71	0.53%	27.66
FDR	32.47	7.31	1.49%	99.64
FDRM	3.80	3.30	0.46%	32.95

Table 8
Quality parameters due to a step in wind power production.

Criteria	Quality parameters			
	$\overline{\sum \varepsilon_n^2} \times 10^{-4}$	$\overline{\sum \epsilon_p^2} \times 10^{-4}$	$desv_{n,max}{}^{-}$	$T_{2\%}{}^{n}$ (s)
Paynter	12.32	5.00	−10.09%	177.63
DCP	9.62	6.84	−10.09%	63.77
FDR	12.22	4.84	−10.07%	133.34
FDRM	11.12	7.74	−10.55%	78.25

In Ref. [34] it is stated that to check the suitability of a controller adjustment it is sufficient to simulate a step, a ramp and a random signal. In this way all possible scenarios are considered.

In order to applying this methodology, three different events, related to wind and solar generation, have been proposed to be simulated and checked. The first one, analogously to the random signal, is taken from wind and solar power generation signals. The second one consists on a wind power output ramp. Both events are assumed as normal operating conditions. Finally, step signal is assumed as abnormal operation conditions; specifically, it consists on a sudden disconnection of a wind farm. Wind/Solar generation is introduced in the simulation model through the "Net Power Demand" block.

In all these cases, the participation of fossil thermal energy is zero.

6.1. Normal operating conditions

6.1.1. Wind and solar power fluctuations

Combinations of three different real scenarios in terms of real production of wind and photovoltaic solar energy have been considered [49]. Due to the unpredictability of these renewable energies, every possible combination of their production levels has been taken into account (9 different scenarios). These power output levels are shown, in per unit values, in Fig. 12.

As an example, Fig. 13 shows the first 500 s of PSHP simulation in the case with high penetration of wind and solar energy. Table 6 summarizes for each scenario, frequency medium square error, power medium square error, maximum positive and negative frequency deviation and minimum pressure downstream of the turbine for each tuning criteria.

6.1.2. Power wind ramp

An event usually considered in isolated systems with high penetration of intermittent energies (wind and solar), is produced by a substantial variation in wind power generation [50]. Here a linear increase in the wind power generated will be considered. Because of this increase in wind generation, the hydro power plant should reduce its production in order to maintain system frequency. Due to the proximity of the proposed wind farm (9 MW) to Garafía (1.6 MW) wind farm (see Fig. 2), wind speed in both wind farms is assumed as equal. The simulated power variation is a 25% of the considered wind farm capacity (10.6 MW) in 60 s (0.053p.u./s). Simulations are shown in Fig. 14. In Table 7 the response quality parameters are shown.

As stated in Table 7, adjustment with less error, frequency overshoot and settling time is FDRM criterion. Fig. 14 shows, as previously explained that there are two types of responses, each one for each pair of tuning criteria.

6.2. Abnormal conditions

A sudden disconnection of the new wind farm (9 MW) is considered as an abnormal situation in the power plant operation. In this case, the hydro plant must increase its generated power in order to compensate for the generation loss in the system and recover the frequency. Fig. 15 shows the hydro power plant response while its quality parameters are shown in Table 8.

In this case, in which two pairs of results are also observed in settling time, both FDRM or DCP present a better performance than the other ones. Despite the fast closing movement in gate position, the safety of pipelines is not compromised due to cavitation phenomena.

Although frequency deviations are within the limits required in Refs. [47], a 10% frequency variation would be inadmissible. In order to correct this undesirable situation two actions have been included in the simulation model: a flywheel, so that T_m is increased in 50% and a load shedding scheme consisting in three load disconnection steps of 2.15, 4.23 and 2.55 MW which are shut down if the frequency is lower than 48.9, 48.8 and 48.5 Hz respectively. The load

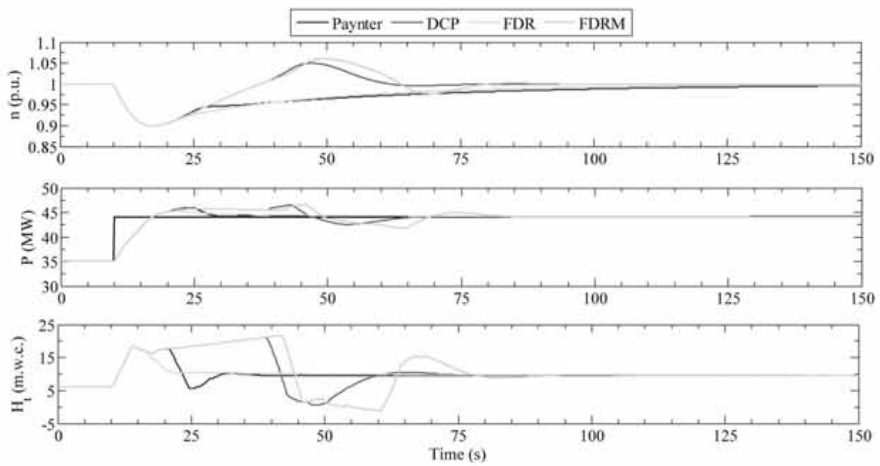

Fig. 15. Hydro plant response due to a power step.

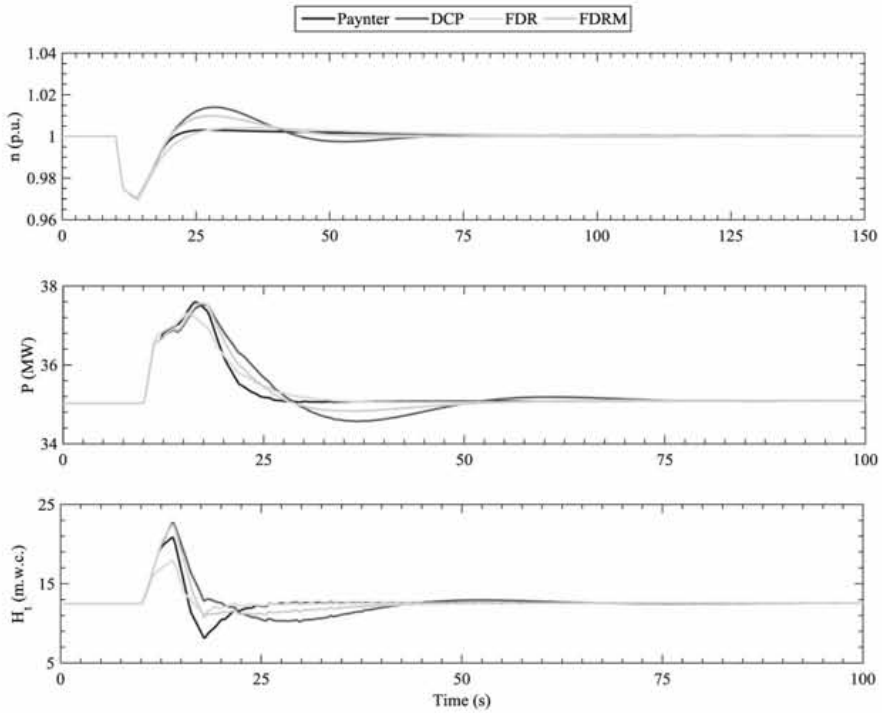

Fig. 16. Hydro plant response due to a power step including an increased inertia ($T_m = 9$ s) and the load shedding scheme.

shedding scheme is taken from other load shedding schemes in similar islands in the Canary Archipelago. Fig. 16 shows the new hydro power plant response while its quality parameters are shown in Table 9. In this case, maximum frequency drop is 3.01% and Paynter criterion is more competitive.

7. Conclusions

In this paper, a model of a hydropower plant with long tail-race tunnel connected to an isolated system with wind and solar energy generation is developed.

It has been considered as a case study La Palma island (Canary archipelago, Spain), where is planned to increase the penetration of renewable sources: wind, solar and pumped storage hydropower. In order to use realistic data in the case study, a pre-design of the pumped-storage hydropower plant has been done, taking into account existing energy expansion plans.

Due to the tail-race tunnel length, cavitation phenomena may appear in response to very fast maneuvers. Thus, it has been necessary to consider water and conduit elasticity in this component, where a continuous elasticity model has been applied. A reduced order model based on lumped parameters has been used for analysis purposes and subsequent development of recommendations for setting the speed controller.

Table 9
Quality parameters due to a step in wind power production step including an increased inertia ($T_m = 9$ s) and the load shedding scheme.

Criteria	Quality parameters			
	$\overline{\sum \epsilon_n^2} \times 10^{-5}$	$\overline{\sum \epsilon_p^2} \times 10^{-4}$	$desv_{n,max}^-$	$T_{2\%}^n$ (s)
Paynter	2.96	3.24	−3.010%	26.37
DCP	4.28	3.52	−3.008%	37.36
FDR	3.29	3.09	−3.003%	40.86
FDRM	3.56	3.38	−3.006%	35.46

A study in the frequency domain has been carried out, obtaining the transfer function of the control loop. Using the root locus technique, it has been derived a setting criterion for the PI controller. Some performance indices have been obtained and compared with those obtained with a classic setting and other criteria developed previously for similar cases. If FDR or Paynter tuning criteria are used, a slow mechanical mode appears in the response, giving rise to much larger settling times than with the other two criteria.

Several simulations have been performed considering realistic cases under normal and abnormal operating conditions, in different scenarios of intermittent (wind and solar) generation. Possible occurrence of cavitation in problematic conduit points has been checked. It has been found that the best performance in all cases is obtained with the proposed controller setting, FDRM.

As a general conclusion is worth noting the feasibility to operate the island power system without the thermal power plants, when there are sufficient solar and wind resources, supplying demand and maintaining the system frequency, without compromising the conduits in the PSHP by cavitation phenomena.

Acknowledgements

The work presented in the paper has been partially funded by the Spanish Ministry of Economy and Competitiveness under the project "Optimal operation and control of pumped-storage hydropower plants" of The National Scientific Research, Development and Technological Innovation Plan 2008 – 2011 (Ref. ENE2012-32207).

Nomenclature

a	pole parameter
a_d	wave speed (m/s) in tail-race
A_t	turbine parameter
b	pole parameter

b_{ij} turbine linear coefficients (p.u.)
c_t turbine mechanical torque (p.u.)
c pole parameter
c_t^0 initial turbine mechanical torque (p.u.)
D turbine parameter
D_d tail-race tunnel diameter (m)
$desv_{n,max}^-$ maximum negative frequency deviation (%)
$desv_{n,max}^+$ maximum positive frequency deviation (%)
D_p penstock diameter (m)
F_d tail-race tunnel section (m^2)
F_p penstock section (m^2)
g gravity acceleration (m^2/s)
G_C controller transfer function
G_{CL} closed loop transfer function
G_{OL} open loop transfer function
H net head (m.w.c.)
h net head (p.u.)
h^0 initial net head (p.u.)
H_b base head (m)
h_c upper reservoir water level (p.u.)
h_d lower reservoir water level (p.u.)
h_p head upstream of the turbine (p.u.)
h_t head downstream of the turbine (p.u.)
$H_t(s)$ head downstream of the turbine in frequency domain (p.u.)
$H_{t,min}$ minimum high pressure downstream of the turbine (m.w.c.)
j $\sqrt{-1}$
k load sensitivity
K_I integral gain in PI governor
K_P proportional gain in PI governor
L_d tail-race tunnel length (m)
L_p penstock length (m)
n frequency (p.u.)
N(s) frequency in frequency domain (p.u.)
n^0 initial frequency (p.u.)
n_{ref} reference frequency (p.u.)
P power (MW)
p_d net demanded power (p.u.)
$P_d(s)$ net demanded power in frequency domain (p.u.)
p_g generated electric power output (p.u.)
$P_g(s)$ generated electric power output in frequency domain (p.u.)
p_g^0 initial generated power (p.u.)
q flow through the turbine (p.u.)
Q_b base flow (m^3/s)
q_d flow at the tail-race tunnel upstream end (p.u.)
$Q_d(s)$ flow at the tail-race tunnel upstream end in frequency domain (p.u.)
q_d^0 initial flow at the tail-race tunnel upstream end (p.u.)
q_{nl} no-load flow (p.u.)
q_p flow at the penstock (p.u.)
$Q_p(s)$ flow at the penstock in frequency domain (p.u.)
q_p^0 initial flow at the penstock (p.u.)
$r_d/2$ continuous head loses coefficient in tail-race tunnel (p.u.)
$r_p/2$ continuous head loses coefficient in penstock (p.u.)
$T_{2\%}^n$ frequency settling time (s)
$T_{ed} = L_d/a_d$ tail-race tunnel water elastic time (s)
T_m generator mechanical starting time (s)
T_{ps} power system starting time (s)
T_r dashpot time constant (s)
T_{wd} tail-race tunnel water starting time (s)
T_{wp} penstock water starting time (s)
v_d water velocity in tail-race tunnel (m/s)
v_p water velocity in penstock (m/s)
z wicket gate opening (p.u.)
Z(s) wicket gate opening in frequency domain (p.u.)
z^0 initial wicket gate opening (p.u.)
$\beta = 8/\pi^2$ correction coefficient
δ temporary speed droop
ζ Damping ratio
λ_i closed transfer unction poles
σ permanent speed droop
$\overline{\sum \varepsilon_n^2}$ frequency mean square error, MSE (p.u.)
$\overline{\sum \varepsilon_p^2}$ power mean square error, MSE (p.u.)

References

J. Kaldellis, K. Kavadias, Optimal wind-hydro solution for Aegean Sea islands' electricity-demand fulfilment, Appl. Energy 70 (2001) 333–354.
J. Kaldellis, K. Kavadias, E. Christinakis, Evaluation of the wind – hydro energy solution for remote islands, Energy Convers. Manage. 42 (9) (2001) 1105–1120.
G. Iglesias, R. Carballo, Wave resource in El Hierro – an island towards energy self-sufficiency, Renew. Energy 36 (2) (2011) 689–698.
J. Merino, C. Veganzones, J. Sánchez, S. Martínez, C. Platero, Power system stability of a small sized isolated network supplied by a combined wind-pumped storage generation system: a case study in the Canary Islands, Energies 5 (2012) 2351–2369.
J. Anagnostopoulos, D. Papantonis, Simulation and size of a pumped-storage power plant for the recovery of wind-farms rejected energy, Renew. Energy 33 (2008) 1685–1694.
S.V. Papaefthymiou, E.G. Karamanou, S.A. Papathanassiou, M.P. Papadopoulos, A wind-hydro-pumped storage station leading to high res penetration in the autonomous island system of Ikaria, IEEE Trans. Sustain. Energy 1 (3) (2010) 163–172.
S.V. Papaefthymiou, V.G. Lakiotis, I.D. Margaris, S.A. Papathanassiou, Dynamic analysis of islands system with wind-pumped-storage hybrid power stations, Renew. Energy 74 (2015) 544–554.
S.V. Papaefthymiou, S.A. Papathanassiou, Optimum sizing of wind-pumped-storage hybrid power stations in island systems, Renew. Energy 64 (2014) 187–196.
T. Ma, H. Yang, L. Liu, J. Peng, Technical feasibility study on a standalone hybrid solar-wind system with pumped hydro storage for a remote island in Hong Kong, Renew. Energy (2014) 7–15.
M.W. Murage, C.L. Anderson, Contribution of pumped hydro storage to integration of wind power in Kenya: an optimal control approach, Renew. Energy 63 (2014) 698–707.
U. Dorji, R. Ghomashchi, Hydro turbine failure mechanisms: an overview, Eng. Fail. Anal. 44 (2014) 136–147.
S. Mansoor, D. Jones, F. Bradley, G. Jones, Reproducing oscillatory behaviour of a hydroelectric power station by computer simulation, Control Eng. Pract. 8 (11) (2000) 1261–1272.
O.F. Jiménez, M. Chaudhry, Stability limits of hydroelectric power plants, J. energy Eng. 113 (2) (1987) 50–60.
C. Sanathanan, Accurate low order model for hydraulic turbine-penstock, IEEE Trans. Energy Convers. 2 (2) (1987) 196–200.
IEEE Working Group, Hydraulic turbine and turbine control models for system dynamic studies, IEEE Trans. Power Syst. 7 (1) (1992) 167–179.
O. Souza Jr., N. Barberi, A. Santos, Study of hydraulic transients in hydropower plants through simulation of nonlinear model of penstock and hydraulic turbine model, IEEE Trans. Power Syst. 14 (4) (1999) 1269–1272.
C. Nicolet, B. Greiveldinger, J.J. Hérou, B. Kawkabani, P. Allenbach, J.-J. Simond, F. Avellan, High-order modeling of hydraulic power plant in islanded power network, IEEE Trans. Power Syst. 22 (4) (2007) 1870–1880.
X. Liu, C. Liu, Eigenanalysis of oscillatory instability of a hydropower plant including water conduit dynamics, IEEE Trans. Power Syst. 22 (2) (2007) 675–681.
K. Naik, P. Srikanth, P. Negi, IMC tuned PID governor controller for hydro power plant with water hammer effect, Procedia Technol. 4 (2012) 845–853.
N. Kishor, R. Saini, S. Singh, A review on hydropower plant models and control, Renew. Sustain. Energy Rev. 11 (5) (2007) 776–796.
S. Hagigara, H. Yokota, Stability of a hydraulic turbine generating unit controlled by P.I.D. governor, IEEE Trans. Power Apparatus Syst. 98 (6) (1979) 2294–2298.
L. Wozniak, a graphical approach to hydrogenerator governor tuning, Trans. Energy Convers. 5 (3) (1990) 417–421.
P. Kundur, Power System Stability and Control, Mc Graw Hill, New York (USA), 1994.
M. Abdolmaleki, A. Ranjbar, P. Ansarimerh, S. Borjian Boroujeni, Optimal tunning of temporary droop structure governor in the hydro power plant, in: 2nd IEEE International Conference on Power and Energy, Johor Baharu, Malaysia, 2008.
J. Sarasúa, P. Elías, G. Martínez-Lucas, J. Pérez-Diaz, J. Wilhelmi, J. Sánchez, Stability analysis of a run-of-river diversion hydropower plant with surge

tank and spillway in the head pond, Sci. World J. 2014 (2014).
P. Hušek, PID controller design for hydraulic turbine based on sensitivity margin specifications, Int. J. Electr. Power & Energy Syst. 55 (2014) 460–466.
G. Martínez-Lucas, J.I. Sarasúa, J.Á. Sánchez, J.R. Wilhemi, Power-frequency control of hydropower plants with long penstocks in isolated systems with wind generation, Renew. Energy 83 (2015) 245–255.
G. Martínez-Lucas, J.I. Sarasúa, J.R. Wilhelmi, J.Á. Sánchez, "Contribution to load-frequency regulation of a hydropower plant with long tail-race tunnel, in: 2015 IEEE 15th International Conference on Environment and Electrical Engineering, Rome, 2015.
Dirección General de Industria y Energía Gobierno de Canarias, Plan Energético de Canarias, 2007.
K. Vidyanandan, N. Senroy, Primary frequency regulation by deloaded wind turbines using variable droop, IEEE Trans. Power Syst. 28 (2) (2013) 837–846.
Consejería de Empleo, Industria y Comercio, Gobierno de Canarias, Anuario Energético de Canarias 2013, 2014.
Consejería de Empleo, Industria y Comercio, Gobierno de Canarias, Revisión Plan Energético de Canarias (PECAN) 2006-2015, 2012.
IEEE Power & Energy Society, IEEE Guide for the Application of Turbine Governing Systems for Hydroelectric Generating Units, 2014. New York.
D. Jones, S. Mansoor, F. Aris, G. Jones, D. Bradley, D. King, A standard method for specifyng the response of a hydroelectric plant in frecuency-control mode, Electr. Power Syst. Res. 68 (2004) 19–32.
Gesplan, Plan Territorial Especial de Ordenación de Infraestructuras Energéticas de la Isla de la Palma, 2007.
C. Platero, C. Nicolet, J. Sánchez, B. Kawkabani, Increasing wind power penetration in autonomous power systems through no-flow operation of Pelton turbines, Renew. Energy 68 (2014) 515–523.
M. Chaudhry, Applied Hydraulic Transients, 2nd ed., Van Nostrand Reinhold, Nueva York, 1987.
M.-E. Grenier, D. Lefebvre, T. Van Cutsem, Quasi steady-state models for longterm voltage and frequency dynamics simulation, in: Power Tech, 2005 IEEE Russia, St. Petersburg, 2005.
T. Van Cutsem, M.-E. Grenier, D. Lefebvre, Combined detailed and quasi steady-state time simulations for large-disturbance analysis, Int. J. Electr. Power Energy Syst. 28 (9) (2006) 634–642.
C. Nicolet, Y. Pannatier, B. Kawakabani, J.-J. Simond, F. Avellan, Simulation of transient phenomena in Francis turbine, in: International Conference in Hydropower, Waterpower XIII, Buffalo (USA), 2011.
J.I. Pérez-Díaz, J.R. Wilhelmi Ayza, I. Galaso Bajo, J. Fraile-Ardanuy, J.Á. Sánchez Fernandez, O. Castaneda Cabrero, J.I. Sarasúa Moreno, Dynamic response of hydro power plants to load variations for providing secondary regulation reserves considering elastic water column effects, Przeglad Elektrotechniczny 88 (1A) (2012) 159–163.
J.I. Sarasúa, J.I. Pérez-Díaz, J.R. Wilhelmi, J.Á. Sánchez-Fernández, Dynamic Response and Governor Tuning of a Long Penstock Pumped-storage Hydropower Plant Equipped with a Pump-turbine and a DFIG, Energy Convers. Manage 106 (2015) 151–164.
B. Strah, O. Kuljaca, Z. Vukic, Speed and active power control of hydro turbine unit, IEEE Trans. Energy Convers. 20 (2) (2005) 424–434.
C. Vournas, G. Papaioannou, Modeling and stability of a hydro plant with two surge tanks, IEEE Trans. Energy Convers. 10 (2) (1995) 368–375.
G. Munoz-Hernandez, D. Jones, Modelling and Controlling Hydropower Plants, Springer Science & Business Media, 2012.
H. Paynter, A Palimpsest on the Electronic Analogue Art, Philbrik Researches Inc, Boston, 1955.
European Standars EN 50160, Voltage characteristics of electricity supplied by public distribution networks, 2007.
Warnick, Hydropower Engineering, 1984.
K. Wada, A. Yokoyama, Load Frequency Control Using Distributed Batteries on the Demand Side with Communication Characteristics, 2012. Berlín.
C. Nicolet, Y. Pannatier, B. Kawkabani, A. Schwery, F. Avellan, J.-J. Simond, Benefits of variable speed pumped storage units in mixed islanded power network during transient operation, in: 16th Annual Hydro Conference, Lyon, France, 2009.